

Electronic Supplemental Information for

**Achieving Long-Lived White Circularly Polarized Luminescence from
Carbonized Polymer Dots via Phosphorescence Resonance Energy Transfer**

Feixiang Wang, Yijie Wang, Rui Guo, Yushuang Wu, Shengju Zhou,* Haibin Xiao*

and Xiaofeng Sun*

School of Chemistry and Chemical Engineering, Shandong University of Technology,
Zibo, 255000, P. R. China.

Author to whom correspondence should be addressed, E-mail:

shengjuzhou@sdut.edu.cn (Shengju Zhou); haibinxiao@sdut.edu.cn (Haibin Xiao);

xiaofengsun@sdut.edu.cn (Xiaofeng Sun)

Experimental

Materials

All chemical chemicals were used directly without further purification. Sodium alginate, L-lysine, sodium fluorescein (Fluc) and sulforhodamine 101 (SR101) were purchased from Aladdin Chemicals Co. Ltd (Shanghai, China). Deionized water was used in all experiments and obtained from a Millipore water purification system (Milli-Q, Millipore).

Synthesis of CPDs

Sodium alginate (0.8 g) was dissolved in 4 mL deionized water and L-lysine (3.2 g) was dissolved in 4 mL deionized water. The above two solutions are mixed and stirred uniformly. The mixed solution was transferred to a poly (tetrafluoroethylene) (Teflon)-lined autoclave (25 mL) and heated for 10 h under 120 °C. After that, the reactor was cooled down to room temperature. The obtained solution was dialyzed in dialysis bag (1000 Da) against deionized water to remove small molecules. Solid CPDs could be obtained via freeze-drying.

Preparation of green afterglow films (CPDs/Fluc)

CPDs (10 mg) was dispersed in PVA aqueous solutions (2 mL) and then stirred for 2 h. After that, different amounts of Fluc stock solutions (5 mg mL⁻¹) was added to the PVA solutions of CPDs. Then, the mixed solution was subjected to ultrasonication for 2 h. The afterglow films were obtained after drying at 80 °C for 3 h.

Preparation of red afterglow films (CPDs/SR101)

The Fluc was replaced with SR101 and the synthesis followed the method of

synthesizing CPDs/Fluc film.

Preparation of white afterglow films (CPDs/Fluc/SR101)

CPDs (10 mg) was dispersed in PVA aqueous solutions (2 mL) and then stirred for 2 h. After that, 0.025 mL Fluc solutions (5 mg mL^{-1}) was added to the PVA solutions of CPDs. Then, different amounts of SR101 stock solutions (5 mg mL^{-1}) was added to the mixed solution and stirred for 1 h. Then, the mixed solution was subjected to ultrasonication for 2 h. The afterglow films were obtained after drying at $80 \text{ }^{\circ}\text{C}$ for 3 h.

Characterizations

The high resolution transmission electron microscopy (HR-TEM) images were recorded on JEOL 2100 system. Raman spectra were collected by laser micro-Raman spectroscopy. X-ray diffraction (XRD) patterns were obtained by a PANalytical X'Pert Powder diffractometer (PANalytical, Holland) with $\text{Cu K}\alpha$ radiation. X-ray photoelectron spectroscopy (XPS) data were collected by an X-ray photoelectron spectrometer (ESCALAB 250). The FT-IR spectrum was obtained by a VERTEX-70/70v FT-IR spectrometer. The absorption spectra were collected by a Shimadzu UV-2600 spectrophotometer. Afterglow decay curves and photoluminescence spectra were measured by a Edinburgh FS5 fluorescence spectrofluorometer. Circular dichroism (CD) spectra were measured on a JASCO J-1500 instrument. Circularly polarized luminescence (CPL) spectra were measured by a JASCO CPL-200.

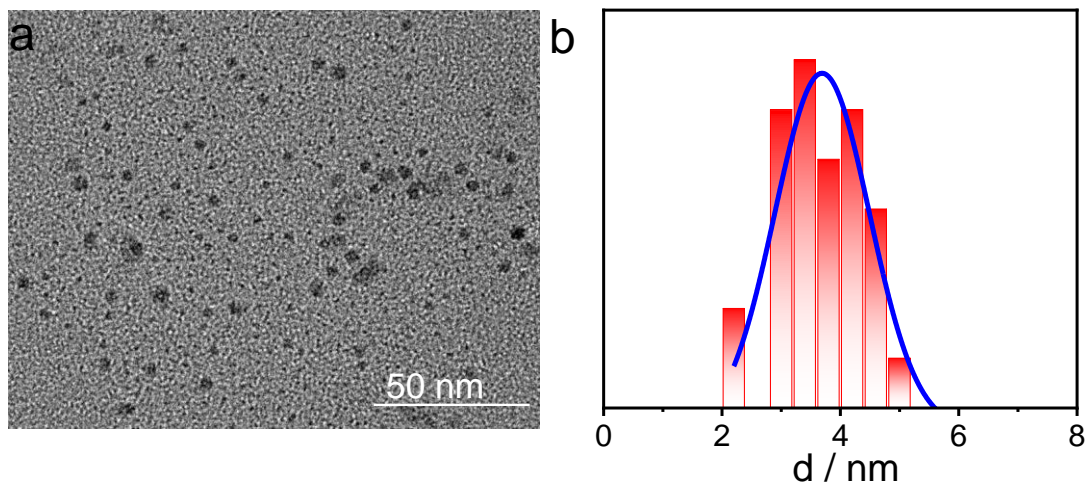


Fig. S1 (a) HR-TEM image of CPDs. (b) Size distribution histogram of CPDs.

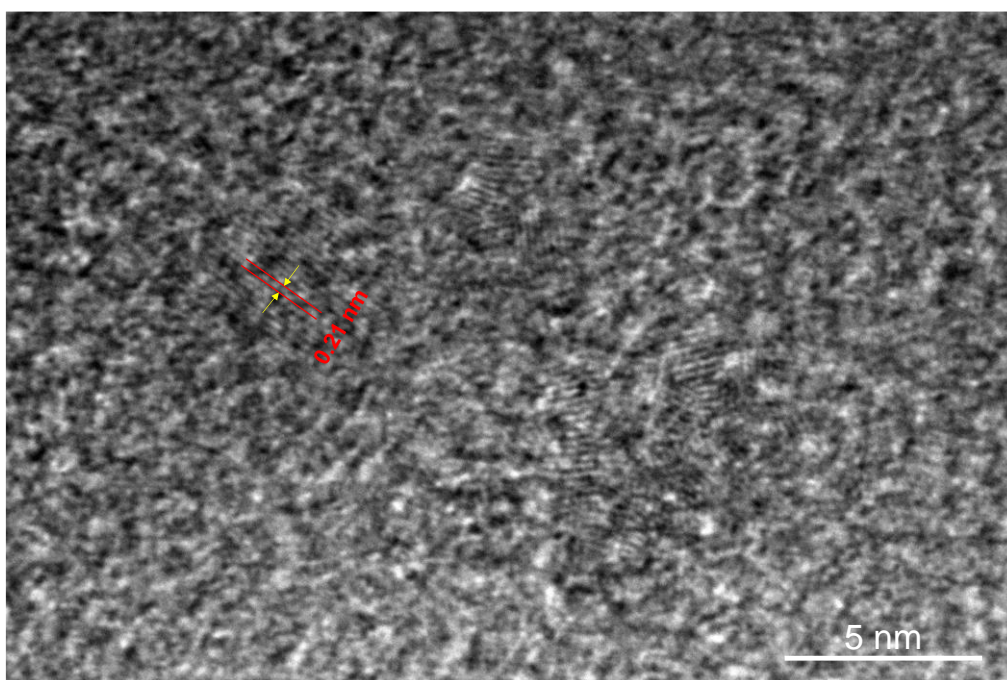


Fig. S2 HR-TEM image and lattice spacing of CPDs.

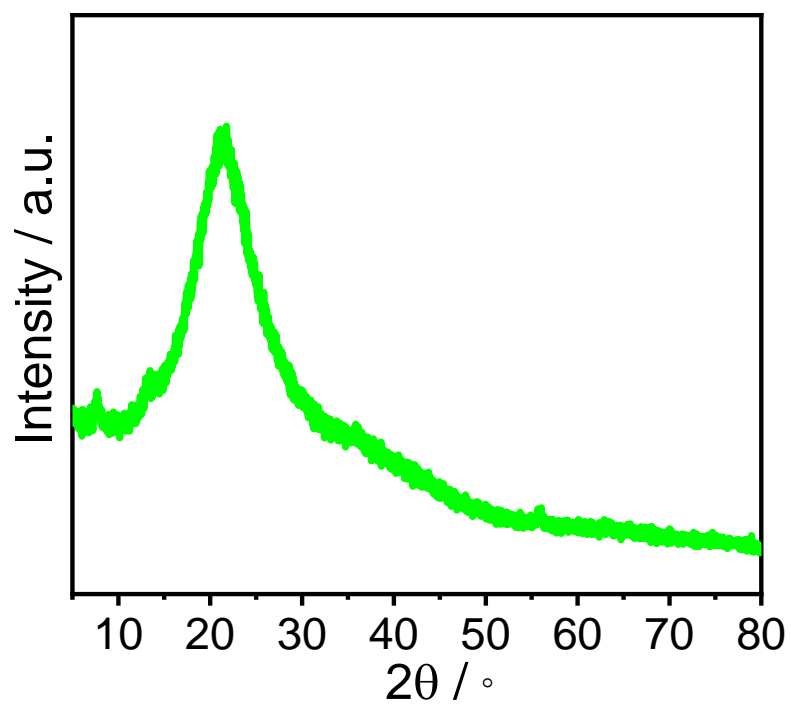


Fig. S3 XRD pattern of CPDs.

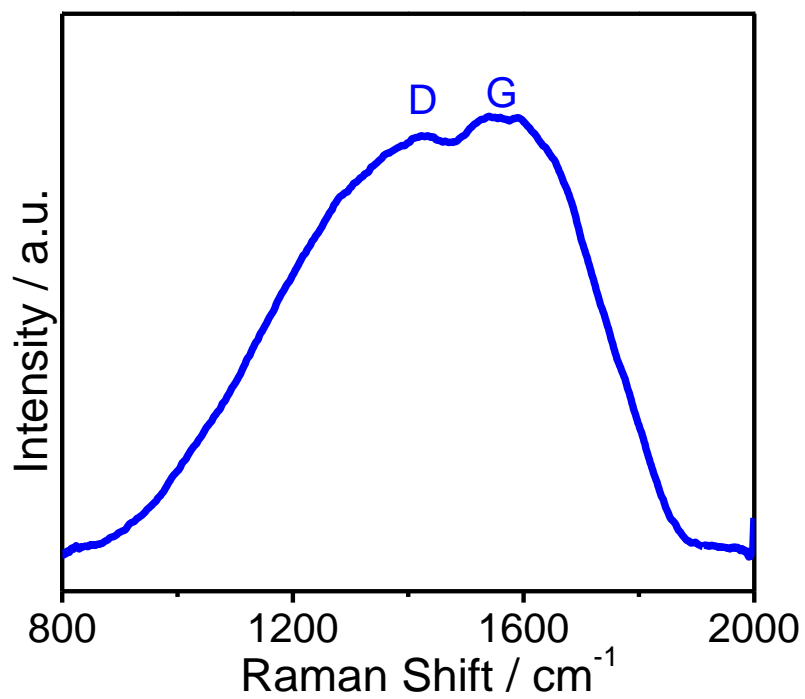


Fig. S4 Raman spectrum of CPDs.

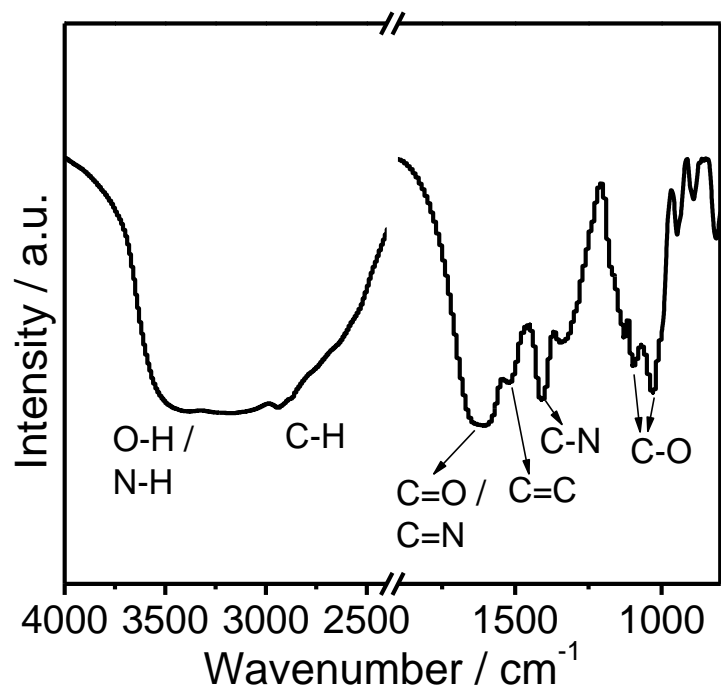


Fig. S5 FT-IR spectrum of CPDs.

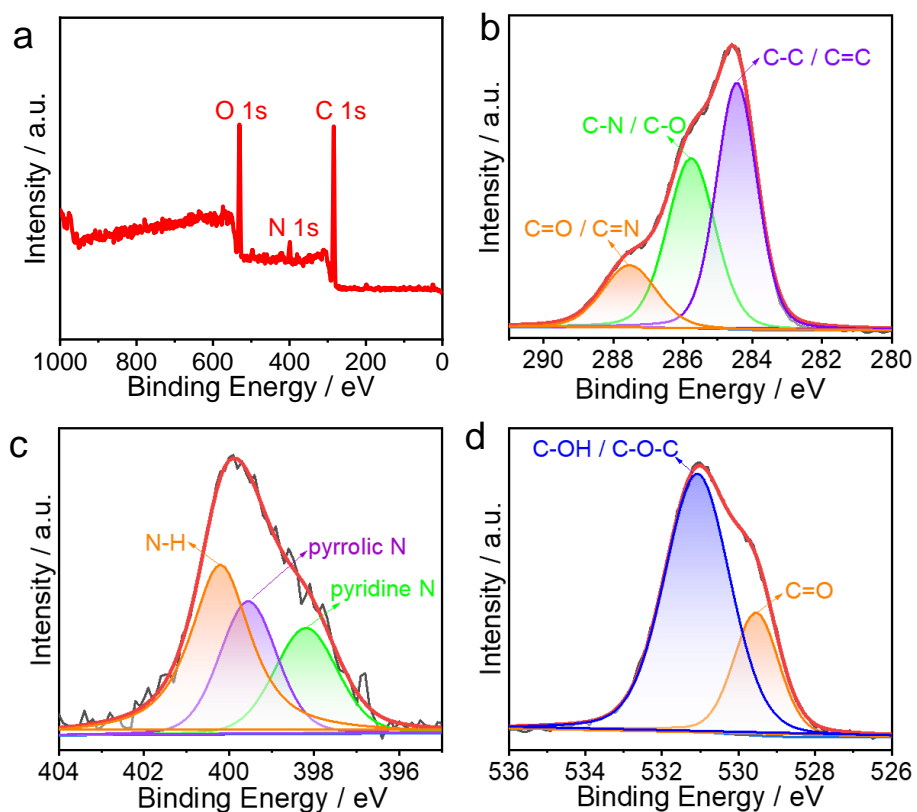


Fig. S6 (a) XPS survey spectra of CPDs. High-resolution XPS C 1s spectra (b), N 1s spectra (c), O 1s spectra (d) of CPDs.

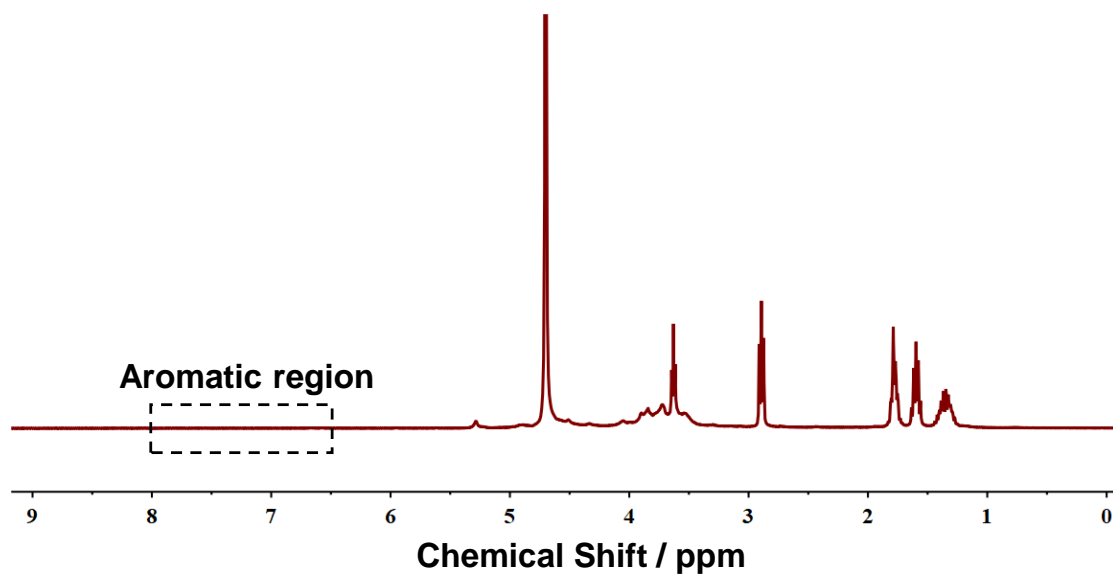


Fig. S7 ^1H NMR spectrum of CPDs.

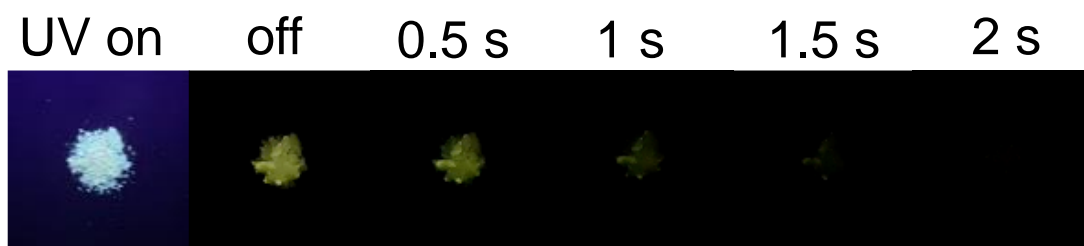


Fig. S8 Photographs of CPDs powder taken under a UV lamp (365 nm) on and off, respectively.

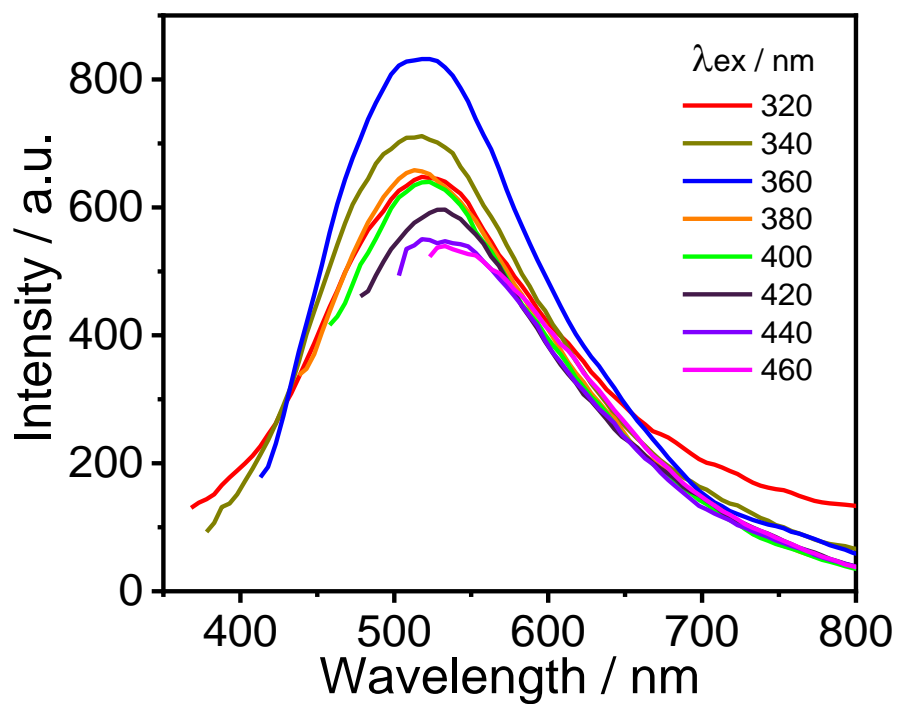


Fig. S9 Phosphorescence spectra of CPDs at the different excitation wavelengths.

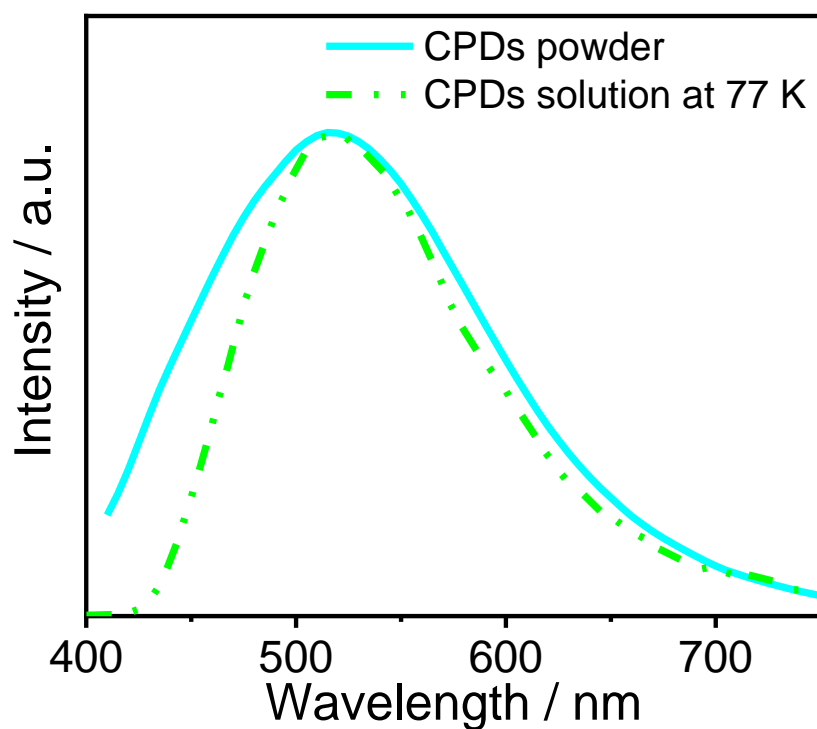


Fig. S10 The RTP emission spectra of CPDs powder and CPDs solution at 77 K excited at 360 nm.

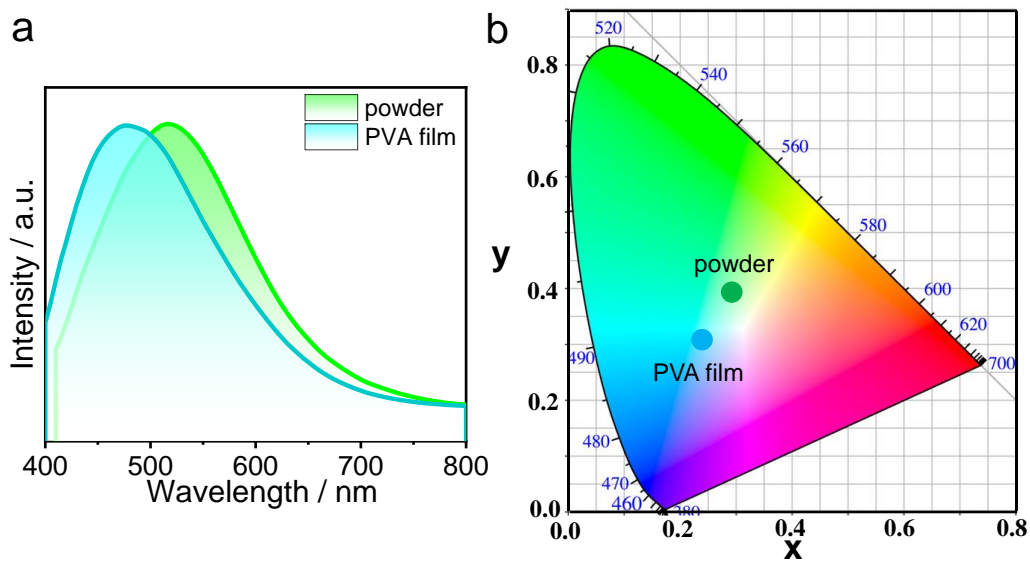


Fig. S11 The RTP emission spectra (a) and CIE chromaticity coordinates (b) of CPDs powder and CPDs PVA film excited at 360 nm.

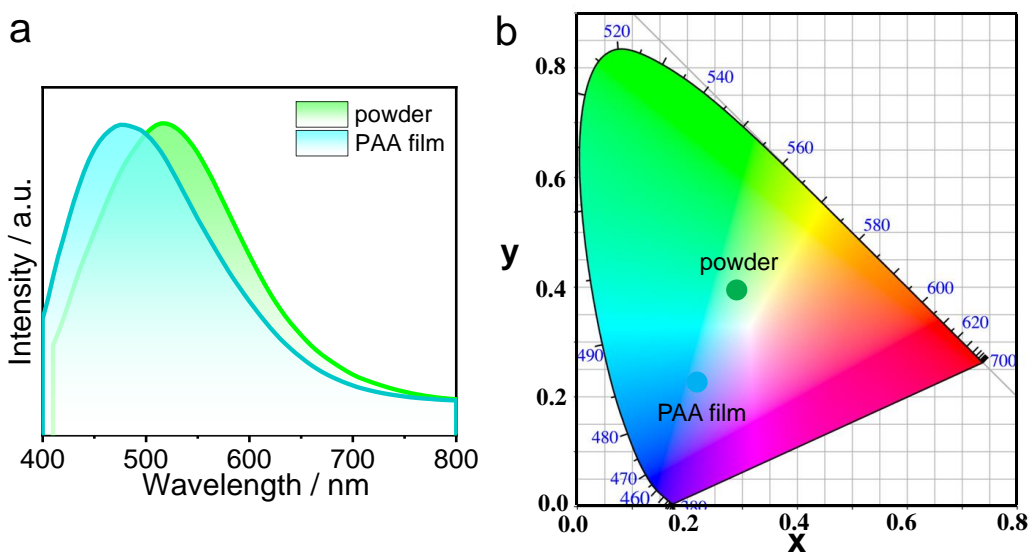


Fig. S12 The RTP emission spectra (a) and CIE chromaticity coordinates (b) of CPDs powder and CPDs PAA film excited at 360 nm.

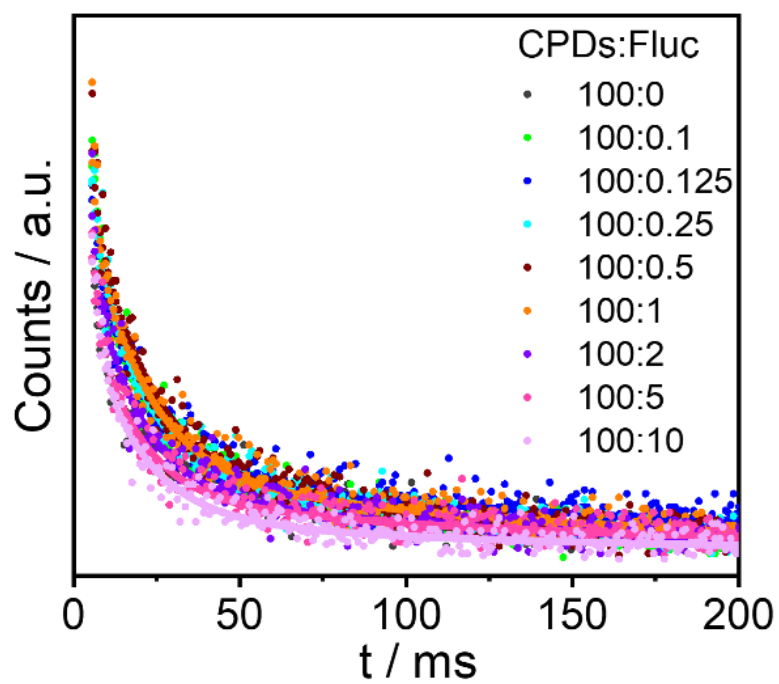


Fig. S13 Afterglow decay monitored at the donor of CPDs-Fluc codoped PVA films.

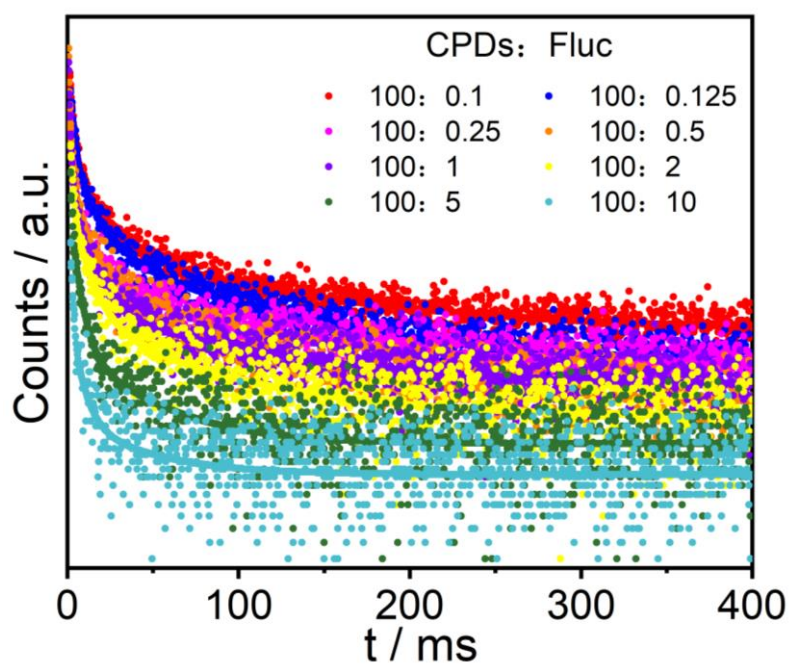


Fig. S14 Afterglow decay monitored at the acceptor of CPDs-Fluc codoped PVA films.

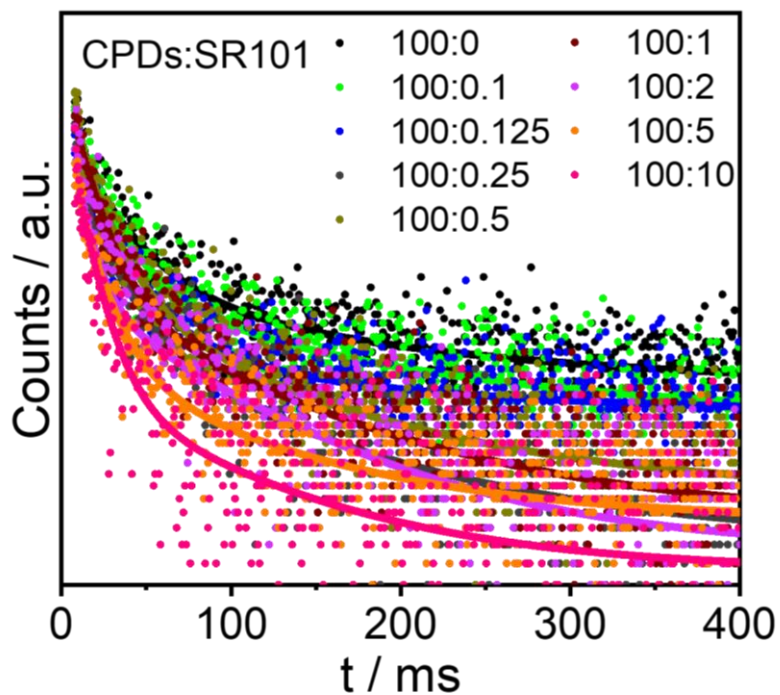


Fig. S15 Afterglow decay monitored at the donor of CPDs-SR101 codoped PVA films.

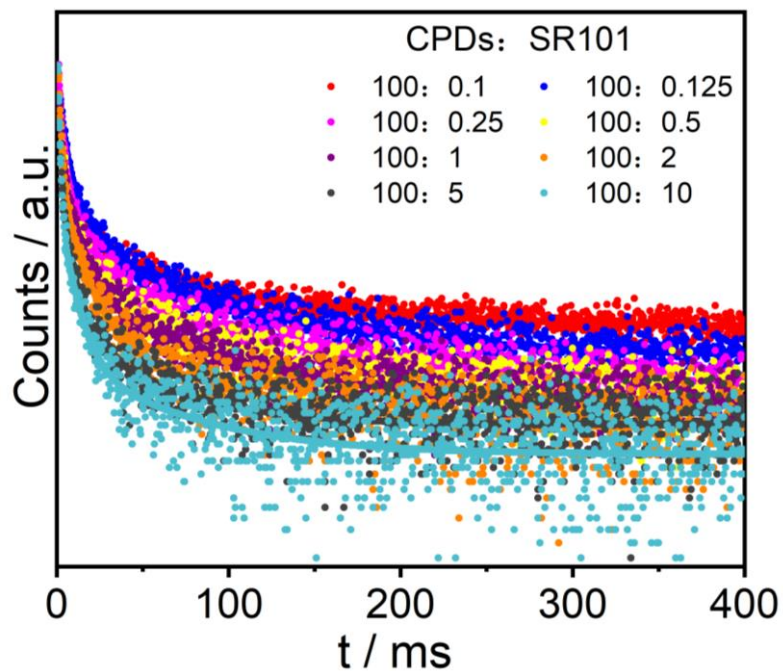


Fig. S16 Afterglow decay monitored at the acceptor of CPDs-SR101 codoped PVA films.

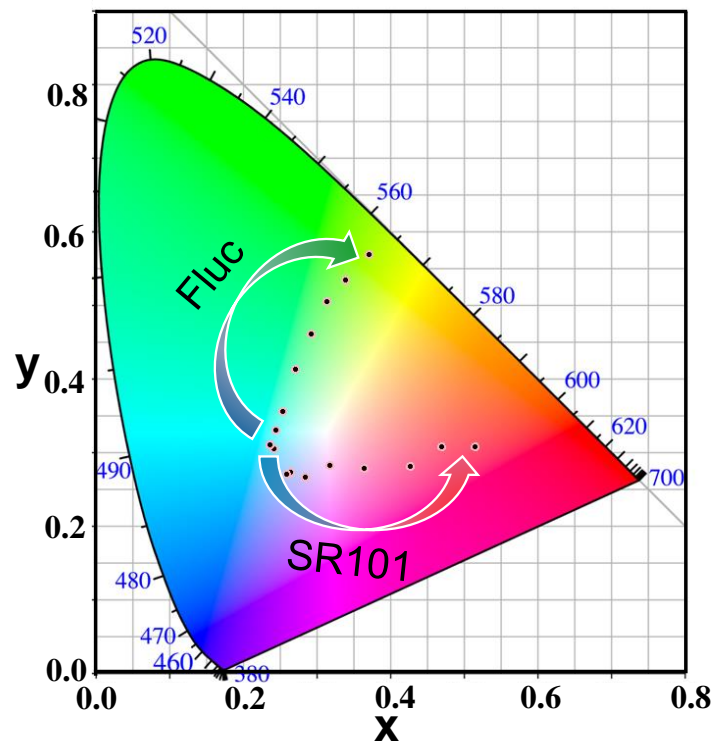


Fig. S17 CIE chromaticity coordinates of CPDs-Fluc/CPDs-SR101 codoped PVA films at different doping weight concentrations.

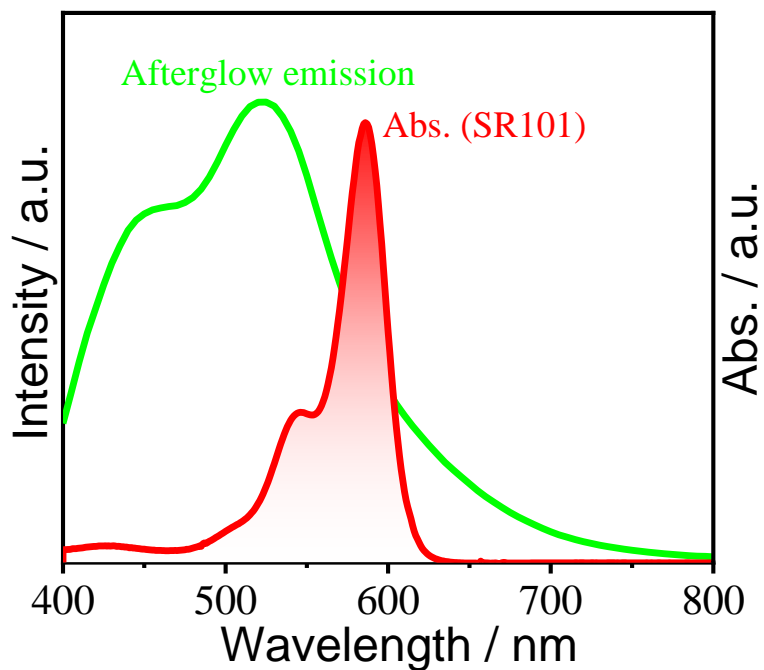


Fig. S18 Overlapped afterglow emission spectrum of energy donors (CPDs/Fluc) and absorption spectrum of energy acceptor (SR101).

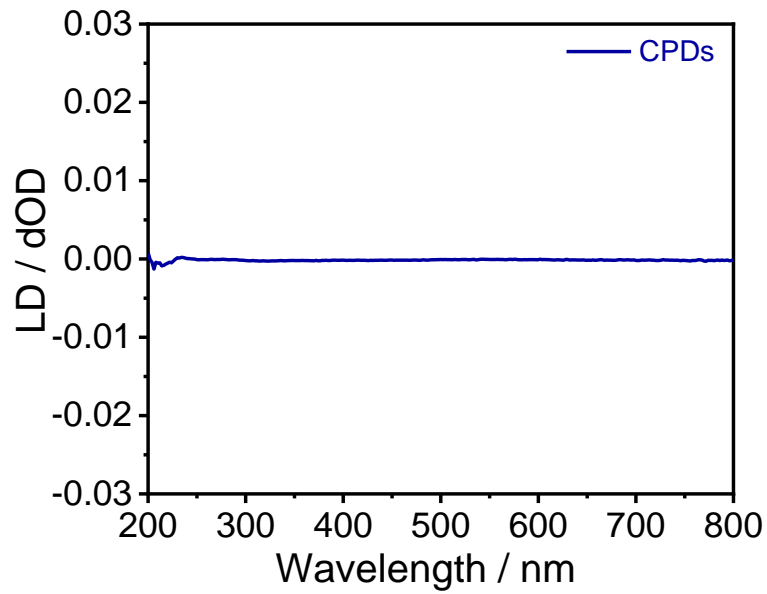


Fig. S19 Linear polarization of the CPDs PVA film.

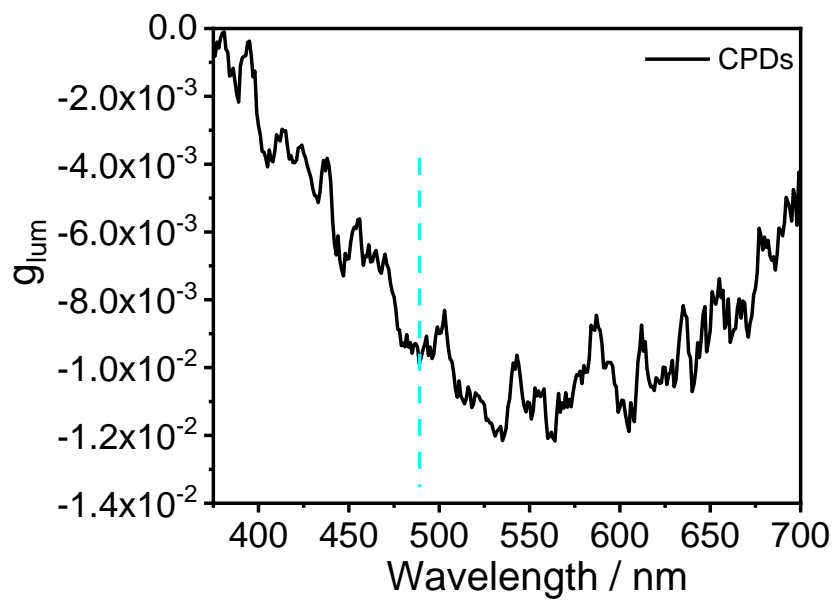


Fig. S20 CPL g_{lum} spectrum of the CPDs PVA film.

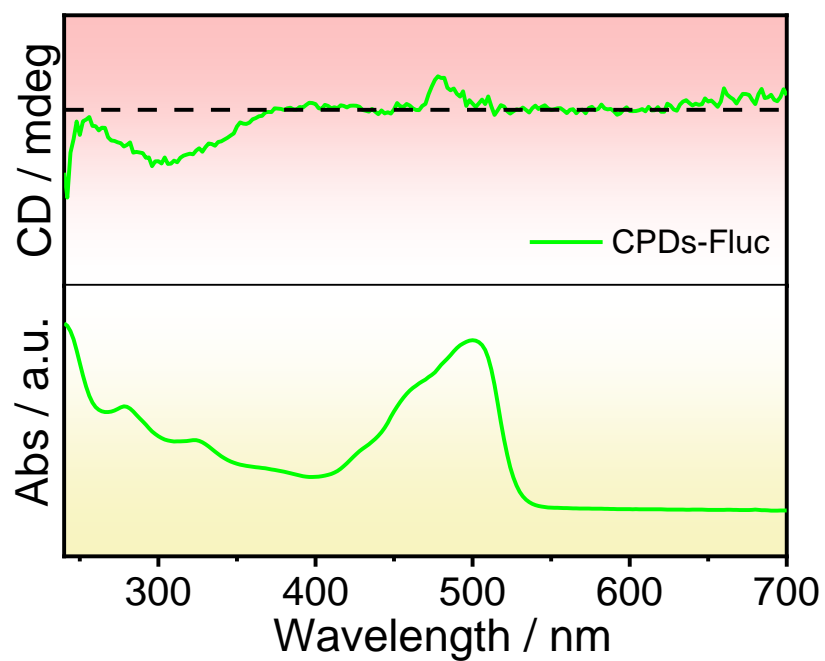


Fig. S21 CD and UV-vis spectra of CPDs-Fluc codoped PVA film.

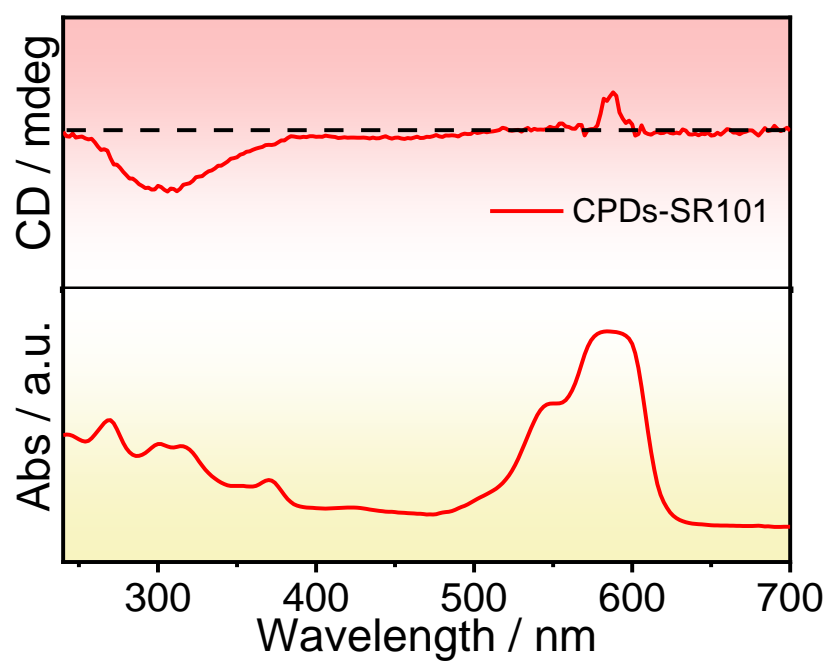


Fig. S22 CD and UV-vis spectra of CPDs-SR101 codoped PVA film.

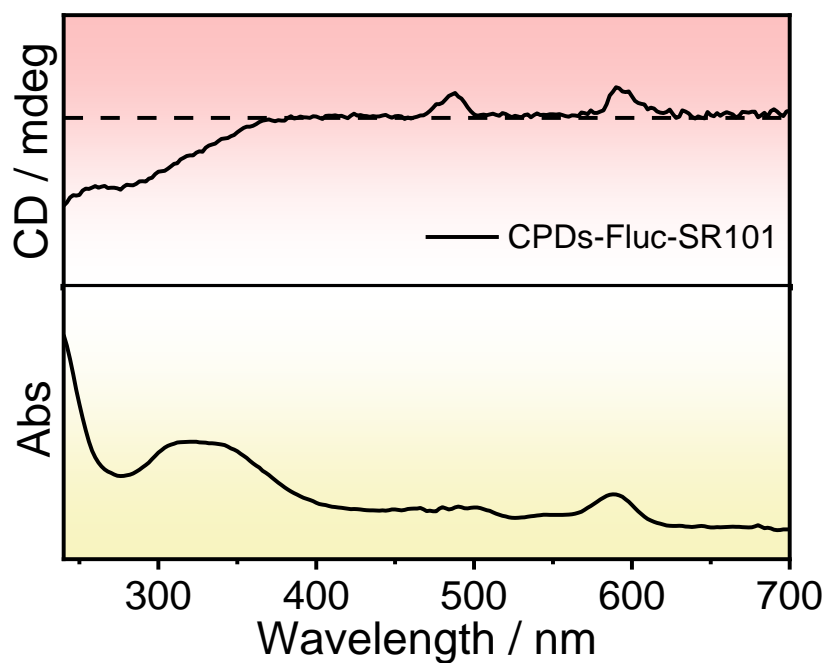


Fig. S23 CD and UV-vis spectra of CPDs-Fluc-SR101 codoped PVA film.

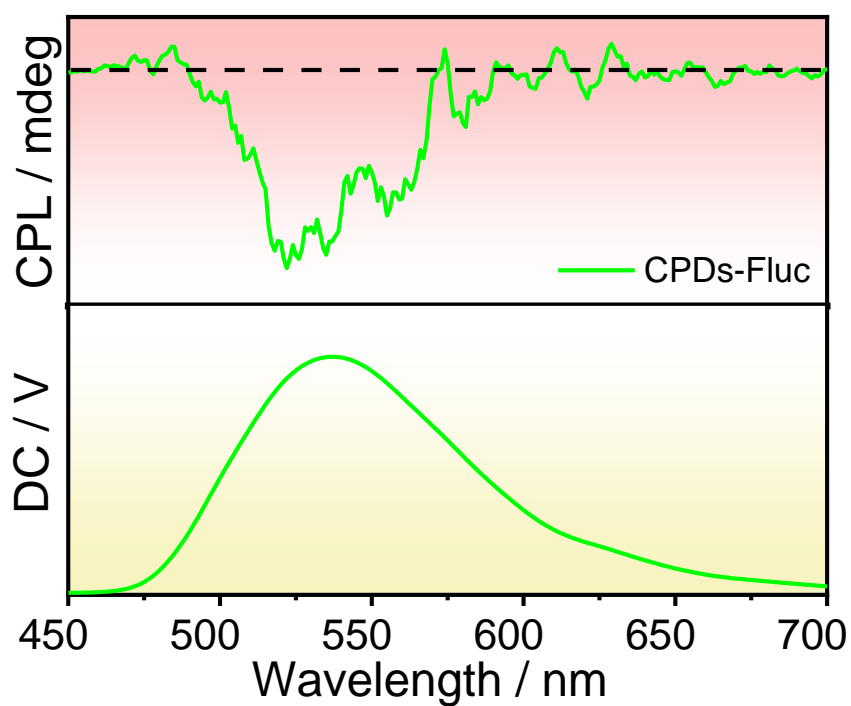


Fig. S24 CPL spectra of CPDs-Fluc codoped PVA film.

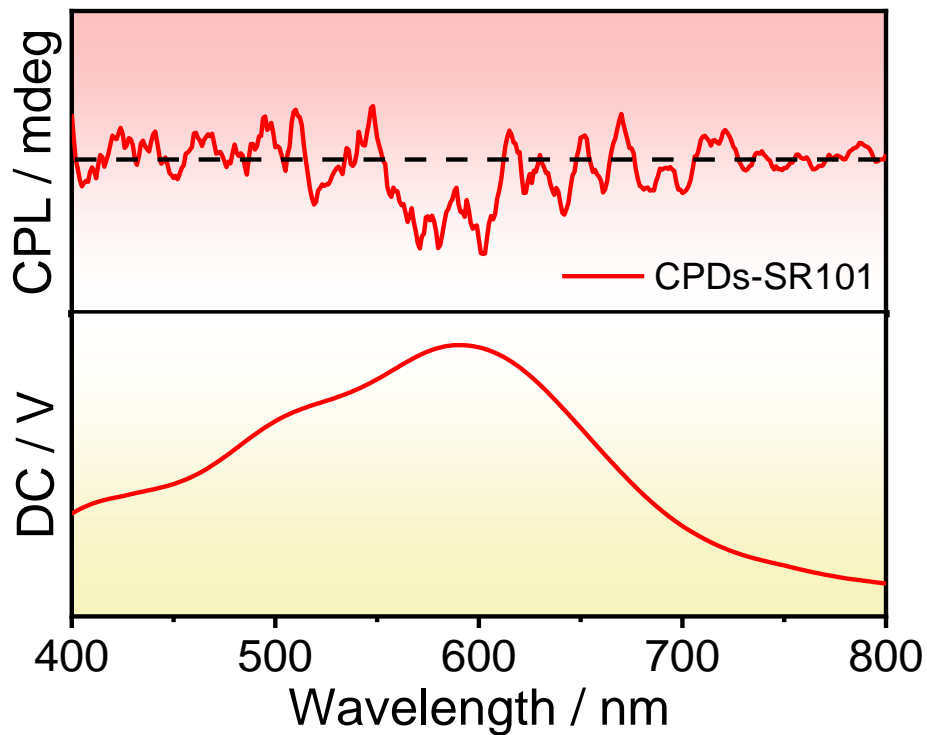


Fig. S25 CPL spectra of CPDs-SR101 codoped PVA films.

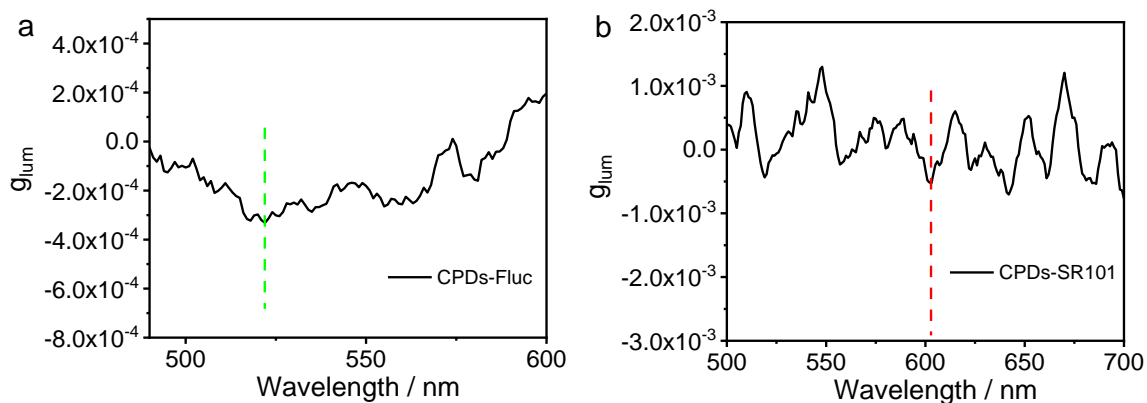


Fig. S26 CPL g_{lum} spectra of CPDs-Fluc codoped PVA film (a) and CPDs-SR101 codoped PVA film (b).

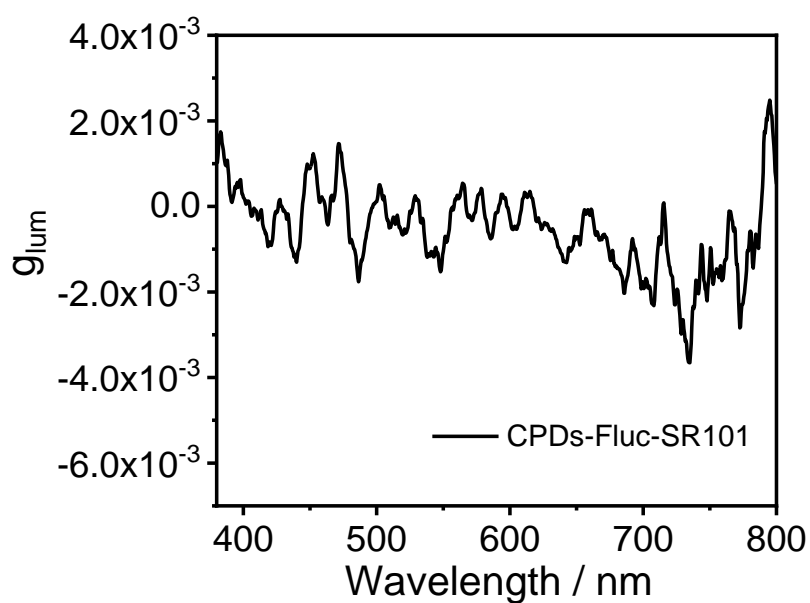


Fig. S27 CPL g_{lum} spectra of CPDs-Fluc-SR101 codoped PVA film.

Table S1. The ΔEst value of the CPDs under different excitation wavelengths.

λ_{Ex} / nm	320	340	360	380	400	420	440
ΔEst (eV)	0.26	0.24	0.25	0.23	0.22	0.20	0.19

Table S2. Fitting parameters of the RTP decay curves of the CPDs powder under excitation at 360 nm.

λ_{Em} / nm	τ_1 / ms	τ_2 / ms	τ_3 / ms	$\langle \tau \rangle / \text{ms}$
517	3.8158 (9.61%)	21.3807 (35.74%)	137.5918 (54.65%)	83.2014

Table S3. Afterglow lifetimes at the donor of the CPDs-Fluc codoped PVA films under excitation at 360 nm.

CPDs: Fluc	λ_{Em}/nm	τ_1 / ms	τ_2 / ms	τ_3 / ms	$\langle\tau\rangle / \text{ms}$
100:0	478	3.9769 (5.43%)	30.3978 (34.66%)	158.8715 (59.91%)	105.9261
100:0.1	478	3.7279 (7.54%)	22.7898 (29.21%)	136.8537 (63.25%)	93.4957
100:0.125	478	1.5207 (17.13%)	16.5046 (25.49%)	146.1467 (57.37%)	88.3174
100:0.25	478	1.4737 (15.12%)	15.0256 (26.33%)	130.9830 (58.55%)	80.8650
100:0.5	478	1.4329 (17.93%)	17.0179 (28.21%)	130.3541 (53.86%)	75.2674
100:1	478	1.5325 (19.80%)	16.6525 (27.83%)	131.1154 (52.37%)	73.5992
100:2	478	1.5425 (21.16%)	14.4212 (28.71%)	122.6303 (50.13%)	65.9406
100:5	478	1.7917 (19.21%)	13.8780 (30.30%)	106.3292 (50.48%)	58.2259
100:10	478	1.9953 (23.66%)	15.9658 (36.57%)	110.3274 (39.77%)	50.1834

Table S4. Afterglow lifetimes at the acceptor of the CPDs-Fluc codoped PVA films under excitation at 360 nm.

CPDs : Fluc	λ_{Em}/nm	τ_1 / ms	τ_2 / ms	τ_3 / ms	$\langle\tau\rangle / \text{ms}$
100:0.1	521	2.0777 (6.71%)	16.4387 (22.97%)	119.396 (70.32%)	87.8755
100:0.125	521	2.2740 (5.78%)	14.0034 (20.22%)	102.0927 (74.00%)	78.5154
100:0.25	521	1.9260 (7.50%)	14.2951 (20.72%)	102.8126 (71.77%)	76.8990
100:0.5	521	1.0397 (9.04%)	10.1496 (23.35%)	97.7169 (67.61%)	68.5322
100:1	521	1.1478 (11.31%)	9.8513 (25.78%)	96.8811 (62.90%)	63.6086
100:2	521	1.5816 (6.83%)	10.2457 (27.17%)	76.2231 (66.00%)	53.2002
100:5	521	0.6899 (5.74%)	5.2699 (31.36%)	42.6888 (62.90%)	28.5434
100:10	521	1.1850 (14.98%)	6.4860 (32.10%)	40.7382 (52.93%)	23.8210

Table S5. Afterglow lifetimes at the donor of the CPDs-SR101 codoped PVA films under excitation at 360 nm.

CPDs: SR101	λ_{Em}/nm	τ_1 / ms	τ_2 / ms	τ_3 / ms	$\langle\tau\rangle / \text{ms}$
100:0	478	3.9769 (5.43%)	30.3978 (34.66%)	158.8715 (59.91%)	105.9261
100:0.1	478	2.5887 (9.11%)	25.0756 (31.33%)	152.4134 (59.56%)	98.8716
100:0.125	478	5.3944 (11.41%)	35.0584 (44.62%)	171.5223 (43.97%)	91.6776
100:0.25	478	3.0175 (11.77%)	27.3486 (29.76%)	134.6705 (58.47%)	87.2377
100:0.5	478	2.7925 (12.80%)	21.6869 (31.13%)	125.5766 (56.07%)	77.5209
100:1	478	1.6216 (19.25%)	17.2033 (27.64%)	127.2909 (53.12%)	72.6809
100:2	478	1.5868 (22.62%)	10.0000 (18.98%)	110.0000 (58.40%)	66.4986
100:5	478	2.2110 (19.05%)	17.3943 (33.06%)	111.0785 (47.90%)	59.3756
100:10	478	1.7514 (20.88%)	14.2976 (33.65%)	106.7063 (45.46%)	53.6889

Table S6. Afterglow lifetimes at the acceptor of the CPDs-SR101 codoped PVA films under excitation at 360 nm.

CPDs: SR101	λ_{Em}/nm	τ_1 / ms	τ_2 / ms	τ_3 / ms	$\langle\tau\rangle / \text{ms}$
100:0.1	621	3.3325 (11.75%)	22.8262 (22.42%)	126.5732 (60.84%)	83.6522
100:0.125	621	3.1845 (8.34%)	16.5905 (25.18%)	97.1469 (66.48%)	69.0249
100:0.25	621	2.1383 (11.70%)	14.4704 (27.40%)	102.0868 (60.89%)	66.3803
100:0.5	621	3.2445 (13.96%)	17.5411 (26.09%)	96.4673 (59.94%)	62.8549
100:1	621	1.2192 (6.04%)	9.4181 (32.19%)	71.7662 (61.77%)	47.4330
100:2	621	1.7009 (16.01%)	12.4512 (36.59%)	88.6783 (47.40%)	46.8607
100:5	621	1.5282 (8.96%)	8.0444 (34.33%)	47.9676 (56.70%)	30.0985
100:10	621	1.1123 (24.56%)	8.5074 (34.77%)	61.3381 (40.67%)	28.1748

Table S7. Afterglow lifetimes at 521 nm of the CPDs-Fluc-SR101 codoped PVA films under excitation at 360 nm.

CPDs: Fluc:SR101	λ_{Em} / nm	τ_1 / ms	τ_2 / ms	τ_3 / ms	$\langle\tau\rangle$ / ms
100:0.25:0	521	1.5529 (18.64%)	17.6924 (27.80%)	137.3650 (53.56%)	78.7812
100:0.25:0.025	521	1.4824 (18.04%)	15.2880 (25.16%)	122.5097 (56.81%)	73.7050
100:0.25:0.0625	521	1.9549 (14.00%)	14.5209 (25.72%)	106.4758 (60.29%)	68.1997
100:0.25:0.125	521	1.6203 (19.42%)	14.6339 (29.36%)	110.0000 (51.22%)	60.9518
100:0.25:0.1875	521	1.5114 (21.21%)	13.1690 (25.31%)	96.3568 (53.48%)	55.1857